J. Phys.: Condens. Matter **12** (2000) 3661–3670. Printed in the UK PII: S0953-8984(00)09445-5

Displacive phase transitions and spontaneous strains in oxygen deficient $CaFe_xTi_{1-x}O_{3-x/2}$ perovskites ($0 \leqslant x \leqslant 0.40$)

A I Becerro†, F Seifert†, R J Angel†, S Ríos‡ and C McCammon†

† Bayerisches Geoinstitut, Universität Bayreuth, 95440 Bayreuth, Germany
‡ Department of Earth Sciences, University of Cambridge, Cambridge CB2 3EQ, UK

E-mail: ana-isabel.becerro@uni-bayreuth.de, friedrich.seifert@uni-bayreuth.de, ross.angel@uni-bayreuth.de, rios@esc.cam.ac.uk and catherine.mccammon@uni-bayreuth.de

Received 10 November 1999

Abstract. The symmetry of $CaFe_xTi_{1-x}O_{3-x/2}$ perovskites ($0 \leqslant x \leqslant 0.40$) has been studied by means of room temperature and high temperature x-ray powder diffraction. At room temperature the perovskites undergo at least two displacive phase transitions with increasing Fe content: from the $CaTiO_3$ $Pbnm$ structure to the tetragonal $I4/mcm$ polymorph at $x = 0.205 \pm 0.017$ followed by transformation to the cubic $Pm3m$ structure at $x = 0.251 \pm 0.029$. A strain analysis of the unit cell demonstrates that the orthorhombic to tetragonal transition is first order in character while the tetragonal to cubic one is second order. An *in situ* high temperature XRD study on compositions with $x = 0.109$ and $x = 0.188$ shows that both samples undergo the same set of phase transitions at high temperature as found in the $CaFe_xTi_{1-x}O_{3-x/2}$ samples with increasing Fe content at room temperature. The transition temperatures indicate that the phase boundaries in the temperature–composition phase diagram may be non-linear.

1. Introduction

Phase transitions in ABO_3 perovskites (A = Na, K, Ba, Ca, Pb, La etc, B = Nb, Ta, Ti, Zr, Al etc) are important from several points of view. They are employed as textbook illustrations of structural phase transitions [1]: many of these perovskite materials are cubic above a critical temperature at normal pressures [2–4] and some of them undergo a variety of temperature-induced structural phase transitions. Perovskites display a variety of electronic properties, from the dielectricity of $BaTiO_3$ [5] and the superconductivity displayed by $Ba(Bi_{1-x}Pb_x)O_3$ [6] to the magneto-resistivity of $(La_{1-x}Ca_x)MnO_3$ [7]. The technological applications of these properties make the perovskite structure one of the most important structures in all material science. Finally, the Earth's lower mantle is believed to be composed mainly of $MgSiO_3$-rich perovskite. Recent experimental investigations [8–10] have shown that the properties of silicate perovskites are strongly influenced by the incorporation of minor elements such as Al^{3+} or Fe^{3+} and that the replacement of $Si^{4+} + 0.5\ O^{2-}$ by Fe^{3+}, leading to an oxygen-deficient perovskite, might be important.

In order to address the geosciences and material sciences questions posed above, we have chosen the model system $CaFe_xTi_{1-x}O_{3-x/2}$ which, in addition, shows interesting conductivity properties [1]. Phases synthesized at high temperatures in this system with x between 0 and ∼0.4 were previously described as having a random distribution of oxygen vacancies, whereas for $x > 0.4$ ordering occurs in $(0k0)$ planes in strings parallel to the [101] direction,

0953-8984/00/153661+10$30.00

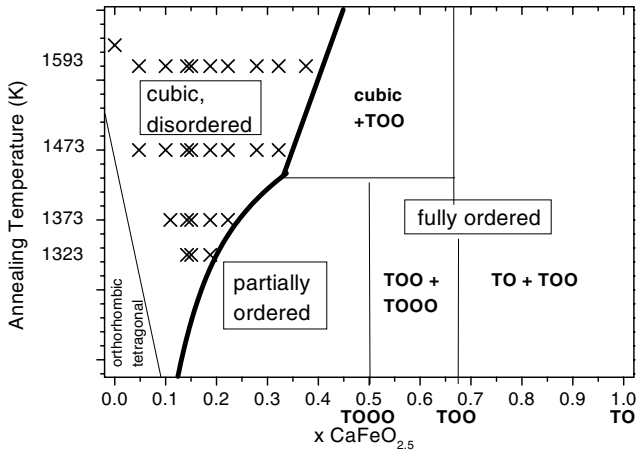

Figure 1. Phase diagram for the system $CaTiO_3$–$CaFeO_{2.5}$ as a function of temperature and composition [13]. Symbols TO, TOO and TOOO indicate the sequence of tetrahedral (T) and octahedral (O) layers in the ordered structures already reported in [27, 28] and [29], respectively. The crosses represent the annealing temperatures and compositions of the samples analysed in this study.

thus creating tetracoordinated sites [12]. A detailed study of oxygen vacancy ordering in this system at different temperatures and Fe contents was reported by us [13] and the phase diagram obtained (representing equilibrium only on a laboratory time scale) is reproduced here in figure 1. In this paper we concentrate on the region of the disordered structures where the number of oxygen vacancies is small (maximum of 6.7% for $x = 0.4$) and, on long length scales, they are randomly distributed in the lattice. The XRD patterns of these samples can therefore be indexed entirely as normal perovskites with orthorhombic, tetragonal or cubic symmetry. By contrast, long-range ordering of the oxygen vacancies gives rise to additional diffraction maxima and inhomogeneous microtextures [14] which were not observed in this study.

The objectives of this study are to determine the symmetry of phases in the system $CaFe_xTi_{1-x}O_{3-x/2}$ (with $0 \leqslant x \leqslant 0.40$) as a function of composition and temperature and to resolve, by means of strain analysis, the order of the displacive phase transitions encountered as a function of Fe content. We have accomplished this using powder x-ray diffraction (XRD) at room temperature. In addition, *in situ* high temperature XRD has been employed to study the influence of Fe^{3+} in the high temperature behaviour of two *disordered* phases, from comparison with the end-member $CaTiO_3$ perovskite.

2. Experiment

Powder samples in the system $CaFe_xTi_{1-x}O_{3-x/2}$, with $0 \leqslant x \leqslant 0.40$, were synthesized from mixtures of $CaCO_3$, TiO_2 and Fe_2O_3, by slow decarbonatization and sintering at 1623 K and repeated intermittent grinding. These materials were then annealed in open AgPd capsules at four different temperatures: 1323 K, 1373 K, 1473 K and 1593 K (figure 1) for periods of 600, 200, 140 and 40 hours, respectively, in CO–CO_2 gas mixtures corresponding to oxygen fugacities one log unit above the iron–wustite equilibrium. Under these conditions all the iron in the samples is present as Fe^{3+}. Samples were then drop-quenched and examined *ex situ* by electron microprobe analysis. Chemical compositions have

been calculated on the basis of two cations per formula unit and are reported as x = mole fraction $CaFeO_{2.5}$.

The symmetry of phases $CaFe_xTi_{1-x}O_{3-x/2}$, with $0 \leqslant x \leqslant 0.40$ was studied by means of room temperature x-ray powder diffraction in a Siemens D-5000 diffractometer with Cu K$\alpha_{1,2}$ radiation. Data were recorded from 20 to 120° 2θ at a scanning speed of 0.02° 2θ min^{-1} and a counting time of 10 seconds. Powdered silicon (NBS) was mixed with the sample to act as an internal standard. *In situ* x-ray diffraction was used to determine the symmetry of the phases with $x = 0.109$ and $x = 0.188$ at high temperatures. The diagrams were collected at increasing temperatures up to 1473 K with different temperature steps. The diffractometer used is described in [15] and employs a curved 120° position-sensitive detector. Powdered α-Al_2O_3, mixed with the sample, was used as an internal standard. All powder diffraction data were analysed using the Rietveld method with the GSAS software [16]. Refined parameters were: lattice constants, line widths, phase fractions and histogram scale factor. Structural parameters were kept fixed at the values for $CaTiO_3$ [17] except that the site occupancies were adjusted to reflect the composition.

3. Results and discussion

3.1. Room temperature XRD study

3.1.1. Symmetry of the phases. The ideal perovskite structure has an ABO_3 stoichiometry and the aristotype has the cubic space group $Pm3m$. Distortions from the ideal cubic structure can be attributed to one of three mechanisms: distortions of the octahedra, cation displacements within the octahedra and tilting of the octahedra. The third distortion mechanism is the most common and can be realised by tilting essentially rigid MO_6 octahedra while maintaining their corner-sharing connectivity. The tilts break the $Pm3m$ symmetry and produce a series of weak superlattice reflections in the diffraction pattern that are diagnostic. These superlattice reflections indicate the space group of the phase [18].

Figure 2 shows the room temperature XRD patterns between 34 and 42° 2θ of a representative set of $CaFe_xTi_{1-x}O_{3-x/2}$ samples previously annealed at 1593 K. The patterns of the samples annealed at the other temperatures are fully consistent with these (and the phase diagram) and are not shown. Each peak contains Cu Kα_1 and Cu Kα_2 contributions. Phases with $x \leqslant 0.188$ show all the superlattice reflections characteristic of the orthorhombic $Pbnm$ space group. For the sample with $x = 0.222$ several observations point to it having higher symmetry (tetragonal $I4/mcm$): (i) both the $\{022, 202\}_{Pbnm}$ and $\{121, 103, 211\}_{Pbnm}$ sets of reflections systematically converge with increasing Fe content, forming single peaks at $x = 0.222$ and (ii) the 021_{Pbnm}, $\{120, 210\}_{Pbnm}$ and $\{121, 103, 211\}_{Pbnm}$ sets of diffractions exhibit a reduction in intensity, the first two being absent at $x = 0.222$ while the third one is still visible at that composition and can be indexed as $211_{14/mcm}$. In the samples with $x \geqslant 0.279$ the $211_{14/mcm}$ reflection has also vanished and the diffraction patterns collected above this composition do not show evidence of any superlattice reflections pointing to a transition to the cubic $Pm3m$ polymorph. Examination of the superlattice reflections indicates, therefore, the following sequence of space groups and transition compositions on increasing Fe content in the system $CaFe_xTi_{1-x}O_{3-x/2}$ ($0 \leqslant x \leqslant 0.40$) at room temperature:

$$Pbnm \xrightarrow{x=0.205\pm0.017} I4/mcm \xrightarrow{x=0.251\pm0.029} Pm3m.$$

The same sequence of phase transitions was described, on increasing temperature, for the $CaTiO_3$ end-member of our system [2], as well as for $SrRuO_3$ [19, 20]. However, Kennedy *et al* [4] suggested that an additional intermediate phase transition from the room temperature $Pbnm$

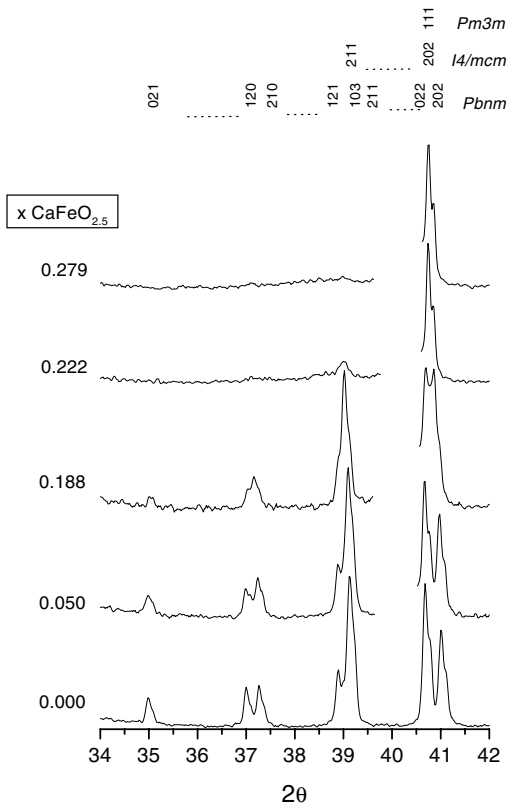

Figure 2. A portion of selected room temperature diffraction patterns of $CaFe_xTi_{1-x}O_{3-x/2}$ showing the composition-dependent splitting of the orthorhombic 022 and 202 reflections as well as the intensity variation of the groups of peaks near $2\theta = 35^\circ$, 37° and 39°. At $x = 0.222$ the reflections near 35° and 37° 2θ have vanished while that near 39° 2θ remains visible, indicating $I4/mcm$ symmetry (as shown by the indices positioned above the patterns). The reflection at 40° 2θ arising from residual Ag–Pd capsule material has been omitted for clarity.

structure to another orthorhombic $Cmcm$ structure occurs on heating $CaTiO_3$. The intermediate $Cmcm$ phase has also been observed in the system $CaTiO_3$–$SrTiO_3$ with increasing Sr content at room temperature [21] as well as in Ca-rich compositions of the same solid solution with increasing temperature [22]. We would therefore expect to see the same sequence with increasing Fe content in our system; however, we did not detect a second orthorhombic phase, $Cmcm$. This might be due to the resolution of our diffractometer being insufficient to resolve the small changes in the diffraction patterns that identify the $Cmcm$ phase [4], or our samples being too widely spaced in composition. Alternatively, the $Cmcm$ phase may not have a stability field at room conditions in this system.

Cell parameters were then refined, by means of the Rietveld refinement method, assuming the space groups mentioned above. Peak splitting for the $Pbnm$ structure could be resolved at all compositions up to the transition to $I4/mcm$, but at higher Fe contents the splitting of the tetragonal peaks in the $I4/mcm$ structure could not be resolved. The lattice parameters for the sample with $x = 0.222$ were, therefore, refined with $a = c$ (metrically cubic). Lattice parameters and unit cell volumes for the samples annealed at 1593 K are given in table 1. Figures 3(a) and (b) display, respectively, the pseudocubic sub-cell parameters and

Table 1. Cell parameters of $CaTi_{1-x}Fe_xO_{3-x/2}$ annealed at 1593 K as a function of x. The tetragonal cell parameters at $x = 0.222$ were refined as cubic since the tetragonal strain was below the resolution of the diffractometer.

x $CaFeO_{2.5}$	a (Å)	b (Å)	c (Å)	Volume (Å^3)	Space group
0.000 (0)	5.3810 (3)	5.4440 (1)	7.6412 (3)	223.815 (7)	$Pbnm$
0.050 (3)	5.3854 (2)	5.4429 (2)	7.6465 (2)	224.134 (9)	$Pbnm$
0.109 (24)	5.3918 (3)	5.4401 (3)	7.6534 (4)	224.429 (16)	$Pbnm$
0.142 (7)	5.3953 (3)	5.4391 (3)	7.6557 (5)	224.658 (15)	$Pbnm$
0.150 (15)	5.3977 (6)	5.4394 (6)	7.6579 (9)	224.833 (24)	$Pbnm$
0.188 (9)	5.4013 (2)	5.4353 (2)	7.6600 (3)	224.876 (8)	$Pbnm$
0.222 (15)	3.8327 (1)			56.301 (2)	$I4/mcm$
0.279 (7)	3.8335 (1)			56.336 (3)	$Pm3m$
0.322 (18)	3.8348 (1)			56.394 (4)	$Pm3m$
0.376 (28)	3.8356 (1)			56.427 (6)	$Pm3m$

pseudocubic sub-cell volume of all of the samples, showing the similarity of the values for the four annealing temperatures. Samples annealed at 1323 K and 1373 K do not show cubic structures due to the intervening order–disorder phase transition (see phase diagram in figure 1). For the orthorhombic phase, the a and c cell edges increase in a nearly linear manner with increasing Fe content while the b axis decreases and all three converge at $x = 0.222$ where the phase transition to tetragonal symmetry occurs. This behaviour is different from that shown by other perovskites with the same set of phase transitions with increasing temperature such as $CaTiO_3$ [2] and $SrRuO_3$ [20]; in these perovskites the three orthorhombic cell edge lengths increase anisotropically in a quasi-linear manner with temperature. This observation suggests that the octahedral tilt responsible for the transition from $Pbnm$ to $I4/mcm$ is driven by different mechanisms with changing composition and temperature. On the other hand, there is little change in volume on transformation from one phase to the other (figure 3(b)) although a change in slope occurs on going from the orthorhombic structures to the cubic ones. Thus, the hypothetical cubic structures at $x < 0.22$ have a higher volume than the orthorhombic structures, a stabilization of the latter being expected with increasing pressure. A similar behaviour is exhibited by the system $CaTiO_3$–$SrTiO_3$ with increasing Sr content at room temperature [21].

3.1.2. Order of the transitions. Orthorhombic perovskites in space group $Pbnm$ have two tilts: an in-phase tilt about the tetrad axis ($[100]_{cubic}$ direction) and a tilt about the diad axis of the oxygen octahedron. The latter is equivalent to two equal out-of phase tilts about the tetrad axes ($[010]_{cubic}$ and $[001]_{cubic}$ directions). In Glazer notation [23] this is $a^+b^-b^-$. In transforming from $Pbnm$ to $I4/mcm$ two of the tilts are removed and there is a single out-of-phase tilt about the tetrad axis ($a^0a^0c^-$). This transition would be first order since it would involve a change in an axis of tilt from the diad to the tetrad axis of the octahedron as well as loss of the in-phase rotation. However, the transformation to the cubic $Pm3m$ space group ($a^0a^0a^0$) could be second order since it only would involve loss of the out-of-phase tilt. The objective of this section is to study the character of the displacive phase transitions that occur in the system $CaFe_xTi_{1-x}O_{3-x/2}$ ($0 \leqslant x \leqslant 0.40$) with increasing Fe content from the point of view of a macroscopic property such as the change in the shape of the unit cell, and compare the results with the symmetry considerations explained above.

The change in shape of the unit cell due to the phase transition is expressed in terms of the *spontaneous strain*, which is defined in terms of the lattice parameters. This quantity

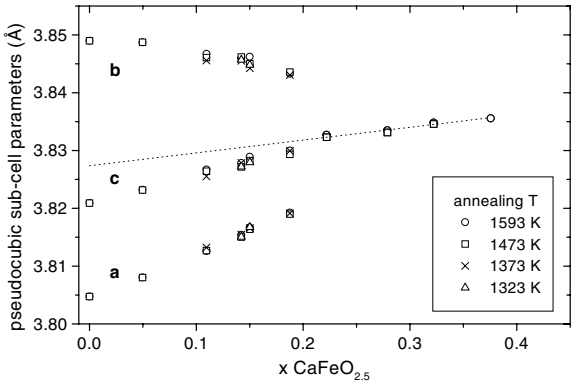

(a)

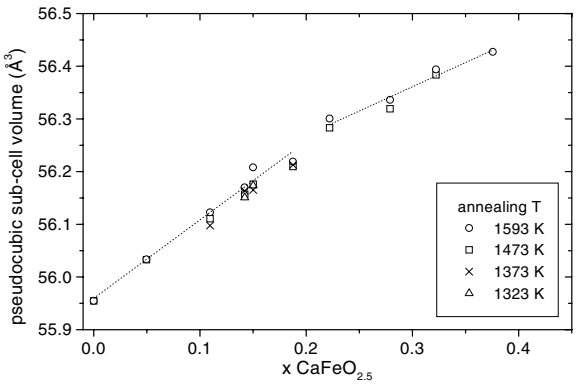

(b)

Figure 3. Compositional dependence at room temperature of (a) lattice parameters and (b) cell volume of $CaFe_xTi_{1-x}O_{3-x/2}$ ($0 \leqslant x \leqslant 0.40$). All parameters are displayed in terms of a primitive pseudo-cubic cell containing one formula unit. The tetragonal diffraction pattern at $x = 0.222$ has been refined as cubic due to the lack of resolution of the experiment. The broken line in (a) is the extrapolation to low Fe contents of the behaviour of the cubic phase and defines the a_0 values. In (b) the broken lines are linear fits to the data points in the ranges $0 \leqslant x \leqslant 0.188$ and $0.222 \leqslant x \leqslant 0.376$.

is always measured relative to the undistorted cell. In the case described in this study the components of the spontaneous strain are defined as: $e_1 = (a - a_0)/a_0$, $e_2 = (b - a_0)/a_0$ and $e_3 = (c - a_0)/a_0$, where a, b and c are the lattice parameters of the orthorhombic phase and a_0 is the lattice parameter that the cubic phase would have at the composition of the orthorhombic phases and is obtained by extrapolation of the cubic parameters. For phase transitions in which the high symmetry phase is cubic and the active representation is doubly degenerate (E), it is often convenient to reduce the number of strain components by expressing them in terms of 'symmetry-adapted' strains [1]. The degenerate symmetry-breaking strains are $e_o = e_1 - e_2$ and $e_t = (2e_3 - e_1 - e_2)/\sqrt{3}$ where the subscript o signifies that e_o is an orthorhombic distortion and the subscript t signifies that e_t is a tetragonal distortion. The factor $1/\sqrt{3}$ is included in the definition of e_t to ensure that the two strains are on the same scale. The symmetry-adapted form of the non-symmetry-breaking strain, e_a, is defined as $e_a = e_1 + e_2 + e_3$.

For the strain analysis we will only consider samples annealed at 1473 K and 1593 K as they are the only ones including cubic structures at room temperature. The symmetry-adapted

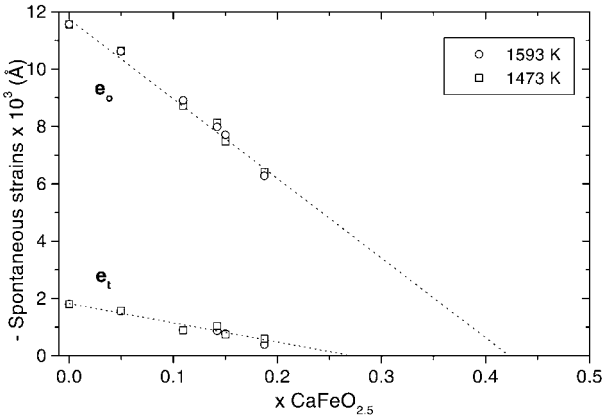

Figure 4. Compositional evolution of the symmetry-adapted strains at room temperature: e_o (orthorhombic strain) and e_t (tetragonal strain) for samples annealed at 1473 K and 1593 K.

strains have been calculated from the lattice parameters of the samples annealed at these two temperatures and plotted against x $CaFeO_{2.5}$ in figure 4. Lattice parameters for the tetragonal phases have not been used; e_a was found to be similar to e_t and has not been plotted for more clarity. Both e_t and e_a are a factor of five smaller than e_o. The evolution of e_t is continuous with composition for both annealing temperatures suggesting that the tetragonal to cubic transition is second order in character with a transition composition of $x \sim 0.26$ as indicated by the extrapolation to zero of the straight line fitted to the data. The transition composition is in agreement with the analysis of the superlattice reflections in section 3.1.1 that placed this transition in the range $x = 0.251 \pm 0.029$. The order of the transition also agrees with the one predicted by symmetry considerations.

On the other hand, a straight line through the data for e_o (figure 4) implies that the orthorhombic distortion would be equal to zero at $x \sim 0.42$. However, the XRD diagrams of the three samples with $0.279 \leqslant x \leqslant 0.376$ did not exhibit any weak superlattice reflections thus indicating that the structure is cubic in this range. This therefore means that e_o must be discontinuous with increasing Fe content and that the orthorhombic to tetragonal transition is first order in character, in agreement with the symmetry considerations. Finally, figure 5 shows the square of e_o against x $CaFeO_{2.5}$ which gives a straight line implying a transition at $x \sim 0.27$. Therefore, if the tetragonal field were suppressed, there would be a direct orthorhombic to cubic transition at that composition that might be tricritical in character although, based on symmetry considerations, the transition should be discontinuous. Another perovskite-type structure, neighborite ($NaMgF_3$), also experiences a direct phase transition from orthorhombic $Pbnm$ to cubic $Pm3m$ on increasing temperature that has been described as tricritical in character [24]. Tricritical phase transitions from tetragonal to cubic symmetry have also been described for $CaTiO_3$ [4] and $SrZrO_3$ [25] on increasing temperature.

3.2. High temperature XRD study

The transition temperatures described in the x-ray diffraction study by Redfern [2] for $CaTiO_3$ perovskite are 1398 ± 25 K for the orthorhombic $Pbnm$ to the tetragonal $I4/mcm$ transition and 1523 ± 10 K for the transformation to the cubic $Pm3m$ polymorph. Kennedy *et al* [4] established by neutron diffraction the transition temperatures to tetragonal and cubic symmetries as 1500 K and 1580 K, respectively, and suggested that there may also be a

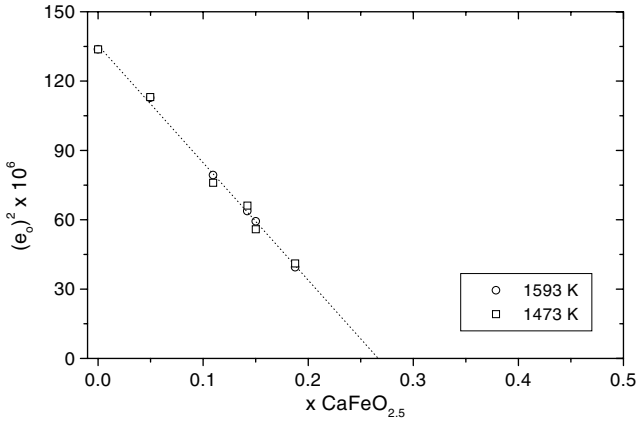

Figure 5. Evolution of the square of the orthorhombic strain with x $CaFeO_{2.5}$ for samples annealed at 1473 K and 1593 K. The broken line implies a tricritical orthorhombic to cubic transition at $x \sim 0.27$.

phase transition from the room temperature $Pbnm$ structure to an orthorhombic $Cmcm$ one at about 1380 K. The same behaviour as that of the $CaTiO_3$ perovskite is expected when small amounts of Ti^{4+} are replaced by Fe^{3+} in the structure of the perovskite, so that the orthorhombic and tetragonal phases that we have reported above at room temperature would be the result of such phase transitions. This has already been postulated in the phase diagram published by us [13] but was at that time unproven.

In order to confirm this assumption and to define approximate transition temperatures, we have collected XRD patterns *in situ* at increasing temperatures of $CaFe_xTi_{1-x}O_{3-x/2}$ compositions with $x = 0.109$ and $x = 0.188$. The *in situ* XRD diagrams were analysed following the same strategy of examining the weak superlattice reflections. The same sequence of phase transitions was found with the following transition temperatures for each composition:

$$\begin{matrix} x{=}0.109: \\ Pbnm \\ x{=}0.188: \end{matrix} \quad \begin{matrix} \text{T(K)}{=}1273{\pm}100 \\ \longrightarrow \\ \text{T(K)}{=}1073{\pm}150 \end{matrix} \quad I4/mcm \quad \begin{matrix} \text{T(K)}{=}1373{\pm}100 \\ \longrightarrow \\ \text{T(K)}{=}1223{\pm}150 \end{matrix} \quad Pm3m$$

Thus, the phases in the system $CaFe_xTi_{1-x}O_{3-x/2}$ that are orthorhombic or tetragonal at room temperature are actually cubic at the synthesis temperatures, but invert upon quenching.

The pseudocubic sub-cell parameters obtained for both samples from the refinements of the high temperature diffractograms are shown in figures 6(a) and (b). As previously found for $CaTiO_3$ [2] the three orthorhombic cell edges increase in a nearly linear manner with temperature and they converge at the phase transition temperatures listed above. Because of the large temperature steps in the *in situ* experiments, the limited resolution in the diffractograms and the uncertainties in the transition temperatures for the $CaTiO_3$ end member ([2, 4]) it is premature to draw definite conclusions on the shape of the temperature–composition phase boundaries, although a non-linear behaviour seems to be suggested. It should be noted, however, that the displacive phase transitions in this system are strongly composition dependent, whereas in the $CaTiO_3$-$SrTiO_3$ system, for example, the temperature–composition curves have much shallower slopes [22].

In order to obtain more precise transition temperatures as well as to determine the extension of the expected 'plateau effect' at very low Fe contents as predicted by Salje *et al* [26], neutron diffraction and calorimetry measurements are planned which will allow a more accurate phase diagram (temperature–composition) of the system $CaFe_xTi_{1-x}O_{3-x/2}$, with $0 \leqslant x \leqslant 0.40$.

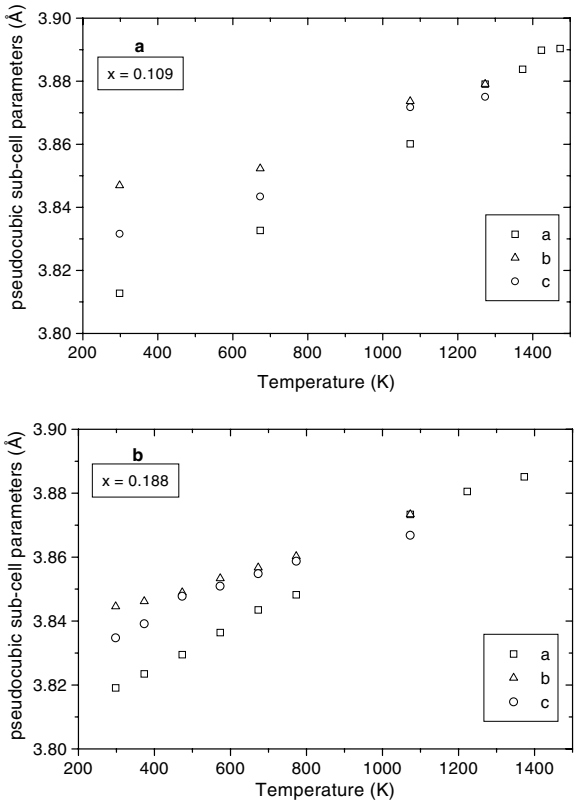

Figure 6. Pseudocubic sub-cell parameters obtained from the refinement of the *in situ* high temperature diffractograms of samples $CaFe_xTi_{1-x}O_{3-x/2}$ (a) $x = 0.109$ and (b) $x = 0.188$. The error bars are half the size of the symbols.

4. Conclusions

Phases in the system $CaFe_xTi_{1-x}O_{3-x/2}$ ($0 \leqslant x \leqslant 0.40$), with randomly distributed oxygen vacancies, undergo at least two displacive phase transitions with increasing x at room temperature: from the $CaTiO_3$ orthorhombic $Pbnm$ to the tetragonal $I4/mcm$ structure at $x = 0.205 \pm 0.017$ followed by transformation to the cubic $Pm3m$ polymorph at $x = 0.251 \pm 0.029$. The data for the orthorhombic strain e_o indicate that the orthorhombic to tetragonal transition is first order, while the evolution of the tetragonal strain with Fe content is consistent with a second-order tetragonal to cubic transition with a transition composition of $x \sim 0.26$. If these two transitions did not occur, there would be an orthorhombic to cubic one at $x \sim 0.27$, tricritical in character. The same sequence of phase transitions found with increasing Fe content at room temperature is shown by the phases with $x = 0.109$ and $x = 0.188$ on heating, the transition temperatures being different for both samples and consistent with a non-linear decrease in transition temperature with increasing Fe content.

Acknowledgments

This research has been possible with financial support from the EU through the TMR Network number ERB-FMRX-CT97-0108. FS also thanks Fonds der Chemischen Industrie for support.

We are grateful to SAT Redfern for useful discussions and to T Abraham for technological support in the high temperature XRD measurements.

References

[1] Putnis A 1992 *Introduction to Mineral Sciences* (Cambridge: Cambridge University Press) pp 260, 404
[2] Redfern S A T 1996 *J. Phys.: Condens. Matter* **8** 8267
[3] Rajeev R and Pandey D 1999 *J. Phys.: Condens. Matter* **11** 2247
[4] Kennedy B J, Howard C J and Chakoumakos B C 1999a *J. Phys.: Condens. Matter* **11** 1479
[5] Galasso F S 1969 *Structure, Properties, and Preparation of Perovskite Type Compounds* (Oxford: Pergamon)
[6] Sleight A W, Gillson J L and Bierstedt P E 1975 *Solid State Commun.* **17** 27
[7] Fontcuberta J, Martínez B, Seffar A, Pinol S, García-Munoz J L and Obradors X 1996 *Phys. Rev. Lett.* **76** 1122
[8] Wood B J and Rubie D C 1996 *Science* **273** 1522
[9] McCammon C 1997 *Nature* **387** 694
[10] Lauterbach S, McCammon C A, von Aken P, Langenhorst F and Seifert F 2000 *Contrib. Mineral. Petrol.* **138** 17
[11] Marion S, Becerro A I and Norby T 1999 *Phase Transitions* **69** 157
[12] Grenier J C, Schiffmacher G, Caro P, Pouchard M and Hagenmuller P 1977 *J. Solid State Chem.* **20** 365
[13] Becerro A I, McCammon C, Langenhorst F, Seifert F and Angel R 1999 *Phase Transitions* **69** 133
[14] McCammon C A, Becerro A I, Langenhorst F, Angel R J, Marion S and Seifert F 2000 *J. Phys.: Condens. Matter* **12** 2969
[15] Salje E K H, Graeme-Barber A and Carpenter M A 1993 *Acta Crystallogr.* B **49** 387
[16] Larson A C and Von Dreele R B 1994 *GSAS: General Structural Analysis System* Los Alamos National Laboratory
[17] Sasaki S 1987 *Acta Crystallogr.* C **43** 1668
[18] Howard C J and Stokes H T 1998 *Acta Crystallogr.* B **54** 782
[19] Chakoumakos B C, Nagler S E, Misture S T and Christen H M 1997 *Physica* B **241** 358
[20] Kennedy B J and Hunter B A 1998 *Phys. Rev.* B **58** 653
[21] Ball C J, Begg B D, Cookson D J, Thorogood G J and Vance E R 1998 *J. Solid State Chem.* **139** 238
[22] Qin S, Becerro A I, Seifert F, Gottsmann J and Jiang J, to be submitted
[23] Glazer A M 1972 *Acta Crystallogr.* B **28** 3384
[24] Carpenter M A, Salje E K H and Graeme-Barber A 1998 *Eur. J. Mineral.* **10** 621
[25] Kennedy B J and Howard C J 1999b *Phys. Rev.* B **59** 4023
[26] Salje E K H, Bismayer U, Wruck B and Hensler J 1991 *Phase Transitions* **35** 61
[27] Colville A A 1970 *Acta Crystallogr.* B **26** 1469
[28] Rodríguez-Carvajal J, Vallet-Regí M, González Calbet J M 1989 *Mater. Res. Bull.* **24** 423
[29] Hovmöller S, Zou X, Neng Wang D, González-Calbet J M and Vallet-Regí M 1988 *J. Solid State Chem.* **77** 316